High-resolution GPR investigation over a Roman mosaic in Empuries, Spain

Alexandre Novo
Head of Product Management GPR Applications
Screening Eagle Dreamlab
Malaga, Spain
alex.novo@screeningeagle.com

Roger Sala
Owner
SOT Archaeological Prospection
Barcelona, Spain
roger_sala_bar@yahoo.es

Manuela Kauffman
Product and Application Expert
Screening Eagle Technologies
Schwerzenbach, Switzerland
Manuela.Kaufmann@screeningeagle.com

Silvia Llobet
ABAC
Barcelona, Spain
silvia@abac-sl.cat

Pedro Rodriguez Simon
PRS Arqueologia
Barcelona, Spain
prsarqueologia@gmail.com

Michael Arvanitis
Head of Product Marketing GPR
Screening Eagle Technologies
Schwerzenbach, Switzerland
michael.arvanitis@screeningeagle.com

2021 11th International Workshop on Advanced Ground Penetrating Radar (IWAGPR) | 978-1-6654-2253-6/21/$31.00 ©2021 IEEE | DOI: 10.1109/IWAGPR50767.2021.9843149

***Abstract*—GPR is a versatile non-invasive method. Although its application in archaeology is widespread, there has been limited research done over historical floors. This paper presents results of how the combined application of high-frequency 3D GPR data acquisition methodologies together with advanced data visualization and complementing ultrasonic scanning is helping conservators in their efforts to protect a Roman mosaic. (*Abstract*)**

Keywords— Ground Penetrating Radar, NDT, cultural heritage, SFCW, archaeology

I. Introduction

The ICOMOS International Committee for Archaeological Heritage Management (ICAHM) has reported that much of the world's archaeological heritage is at risk [1]. This includes not only excavated sites but also monumental structures and small surface sites. One of the reports mentions nearly 1 million monuments and sites and an average of one monument destroyed every day since 1945. Among other reasons (legal, natural, political, cultural), lack of monitoring is impacting to proper assess the risk to archaeological heritage.

During the last two decades, ground penetrating radar (GPR) has been one of the most utilized non-destructive tools in archaeology due to its high-resolution data and 3D visualization capabilities [2, 3]. There are some publications about its use in monitoring of monumental structures [4] but very few to conservation of historical floors [5, 6, 7]. In the last decade, advances in hardware [8] and software [9] have made possible to improve 3D GPR methodologies for archaeological prospection [10].

Currently there is an increasing demand for nondestructive technology to assess and monitor concrete structures due to failing aging infrastructure. Therefore, handheld GPR instruments are routinely used for concrete scanning to detect and map steel reinforcement, tendon cables, and shallow utilities. This has pushed new developments in GPR [11], bringing new opportunities for other fields of application. For example, broader frequency ranges containing frequencies higher than 2-3GHz could be more sensitive to small changes in dielectric at very shallow depths allowing for early defects detection and preventive diagnosis. Also, as shown in previous archaeological investigations on historical floors [12], GPR can be successfully used with other complementary non-destructive technologies.

The subsurface monitoring of ancient floors presents some challenges. On one hand, the fragility of the structure itself composed by tiny, delicate tiles. On the other hand, the complexity of the underlying materials. Therefore, to non-invasively and accurately map these structures, a small, light device with very high-resolution and fast deployment capabilities is needed together with advanced data post-processing software.

We present a multi-technology approach using a novel workflow for non-invasive subsurface mapping applied to monitoring methodologies for conservation of historical floors. The main objective was to understand the causes of deformations at the surface of a damaged Roman mosaic by generating a 3D model of the subsurface layers that composed the structure.

II. The Archaeological Site

Empuries is the only archaeological site on the Iberian Peninsula where there are remains of a Greek and a Roman city at the same place. The Greek occupation started in the 6th century BC. They first occupied the Sant Martí d'Empúries promontory and the land situated south of the natural port where they developed a new center known as Neapolis. After the Romans conquered the Iberian peninsula at the beginning of the 1st century BC they built a new city with a regular plan covering 23 ha. Due to its vast heritage, the site has been surveyed with different geophysical methods over the past years [13, 14, 15].

Roman mosaic at Neapolis

This mosaic (N-S17-2) is composed by ceramic mortar built during the beginning of the first century BC. It is part of a banquet hall at a house situated on the sector 17th, SW of the Greek city. The floor follows a circa 4x3m trapezoidal shape. It preserves its original décor with white tesserae forming a central reticulated rhomboid and an inscription in ancient Greek.
During the 1950s, 60% of the pavement was rebuilt, resulting in the loss of the original materials. Previous studies have documented the original floor's construction

composed by a base layer of locally sourced calcareous stones up to 50mm depth. On top of that, a layer of mortar presenting ceramic fragments ranging from 0.05 up to 20mm. The current conservation state is deficient as it presents structural deformations and damages such as cracks, fractures, small cavities and a big central bulging. That warping creates fractures on the tesserae and is currently the deterioration that concern archaeologists the most (Figure 1).

The conservationists studying the mosaic have two hypotheses for the cause of this problem: 1) The presence of tree roots underneath and 2) Different construction materials and thicknesses of those materials between the original pavement and the reconstructed one. In both cases, the effect would be the generation of small voids that create perfect nests for microorganisms to grow deformations on the mosaic.

Even though shallow roots of a nearby cypress tree were thought to be the main cause, no trace of them has been found in the GPR data within the first 50cm. This is consistent with the results obtained in previous investigations using different GPR instruments in 2017. However, the results from these previous surveys indicate that using a higher resolution GPR may lead to obtain deeper insights of the mosaic's stratigraphy to further investigate the second hypothesis.

III. Methodologies

Geometry of the investigated structure is key for proper GPR data analysis [16]. In this case, a digital elevation model extracted from photogrammetry (Fig. 1) was used to correlate different amplitude responses with actual surface condition of the mosaic.

Fig. 1. Orthophoto (A) showing N-S17-2 mosaic. Shaded relief (B) and countour map (C) images of the topographical model extrated from the orthophoto. Proceq GP8800 GPR system (D) used for this investigation.

The entire mosaic floor was scanned using a Proceq GP8800, a wireless, portable Stepped-Frequency Continuous-Wave (SFCW) GPR with a 400-6000MHz modulated frequency range. It is usually referred to as a 'palm antenna' due to its small size (8.9x8.9x7.6cm). The field workflow started with data acquisition using a tablet that connected to the GPR via WiFi. The GP 5.0 app was used for data acquisition and real-time radargram visualization. A total of 358 line-scans were collected to cover the whole mosaic following XY grids with a 5cm crossline spacing and 1cm inline spacing using a time window of 16ns and 655 samples per scan. Extreme care was taken in order to have very accurate positioning of all lines.

After all grids were collected, they were automatically uploaded to a cloud-based web application for further data management and analytics (Fig. 2).

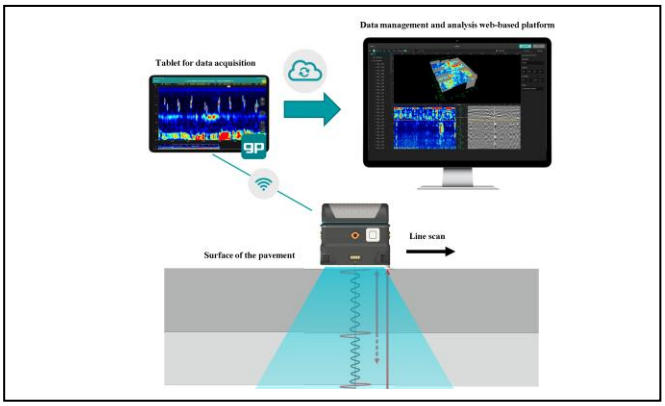

Fig. 2. This diagram shows the workflow used on this investigation. From sensor data acquisition (bottom of the image) to data management and analysis over a cloud based ecosystem.

For advanced GPR data post-processing, a combination of a novel web-based data analysis platform and traditional desktop software was used. First, GPR Insights v1.0 allowed for quick 3D visualization from the field with the same data logger used for data collection. Several filters such as time-zero corrections, bandpass, automatic gain curve (AGC), background removal, 2D migration and Hilbert transform together with slicing and gridding, using inverse distance interpolation algorithms, are built-in and applied in batch for quick access to post-processed radargrams and C-scans. This first visualization helped in data quality assessment as well as the identification of areas of interest.

Secondly, for advanced data visualization and further analysis we used GPR-Slice v7.0. Departing from the same filters sequence, two different 3D cubes were built: One using Hilbert transformed data, which is the most common way of visualizing C-scans due to a more intuitive, simpler image. A second volume was generated keeping the polarity of the phase as this has been proven that small amplitude changes can unveil subtle archaeological features, previously unseen [17]. This technique is called "pulse" or "phase" volume for full-resolution GPR imaging [18] and mostly suggested for densely collected data.

In this case, a cube of 1cm XY cells and 1-sample thick Z cells was compiled to keep the highest image resolution. Blanking areas were filled by interpolating within the

nearest 2 cells for full coverage.

To extract more information about the presence of voids, we collected a profile of ultrasonic (UT) array data over the bulging. Whereas GPR is based on electromagnetic waves, ultrasonic is based on elastic shear waves and are therefore sensitive to different material changes within a structure. For example, elastic waves are highly sensitive to air gaps (up to 99 % of the energy is reflected) whereas the electromagnetic waves can travel through air. We used the Pundit PD8000 system that has a nominal transducer frequency of 40kHz and has 8 channels. The system has point contact transducers that are coupled with the surface by pressing them against it. Once that happened, all transmitting and receiving pairs automatically measured data that are reconstructed to a 21cm wide scan using a synthetic aperture focusing technique (SAFT) [19].

IV. Results

Time-slices were examined to differentiate different materials within the pavement and to study the underlying structures of the original and the rebuilt sections. Images from both, Hilbert and pulsed volumes, shown a clear difference in response of the two pavement areas. Thin depth-slices from the pulsed volume provide the opportunity to detect subtle amplitude changes related to different composite materials between the original part and the reconstructed one. Visualizing animations of these depth-slices can help to understand the complexity of pulsed 3D GPR. Unfortunately, animations are impossible to display on printed documents.

Instead, for an easier representation and more intuitive visualization, we decided to use the most representative slices of the Hilbert transformed data cube and superimposed them to the orthophoto (Fig. 3). Secondly, an overlay analysis technique was applied to represent in a single image the highest amplitude responses at different depth levels (Fig. 4). This approach has been proven helpful in archaeological interpretation of complex material deposition [20].

This together with sections of the Hilbert 3D cube allowed to interpret between different homogeneity levels of pavement layers (Fig. 5). The original segments of the pavement (A) show a stronger reflection at 0.3 nanoseconds or 2cm, in contrast with the lower reflection of the rebuilt surrounding pavement.

The preserved parts of the original pavement (A) appear to lay over a second, less continuously reflective layer, interpreted as the base or statumen, composed by sand and small limestone rocks. That second layer maintains its reflection strength down to 6cm depth, from where it decreases progressively with depth.

Interestingly, at the same depths, the rebuilt pavement shows a much less reflective response until a range of 8-9cm depth. That response is interpreted as a result of a homogeneous filling material, probably sand.

On the original pavement area, under 6-7cm depth, the data still shows a quite high signal amplitude reflection, including some punctual stronger reflectors at 20cm depth. This is interpreted as a sub-base layer which could be composed by compacted sand and limestone rocks.

Apart from these extensive elements, some local anomalies bring relevant information. A linear, reflective feature called B is detected from 4cm to 13cm depth at the edge of the original pavement, probably corresponding to a void of undetermined origin. In a similar range of depths, another linear feature appears in the limit between the two segments of the pavement (G). In that case, the strength of the reflection is slightly weaker than B, but it also appears to relate to a more extensive alteration, called D. This anomaly clearly differs from the response obtained in the rebuilt pavement, pointing to the existence of a flat object placed between 6cm to 9cm under the pavement surface.

The complex geometry of these elements correlates well with the important deformations of the pavement in that area. For example, feature G corresponds with the joint between the ancient and modern materials.

From 11-12cm depth, on the eastern half of the pavement, in the rebuilt area, new changes in the response appear. Several small reflectors, called feature F, appear from the north limit of the pavement, probably corresponding to small limestone rocks in a more continuous media, presumably sand.

In the south-west corner of the pavement, it appears a new reflective feature, E, at 14cm depth. According to its shape and response it could correspond to a small building feature or wall.

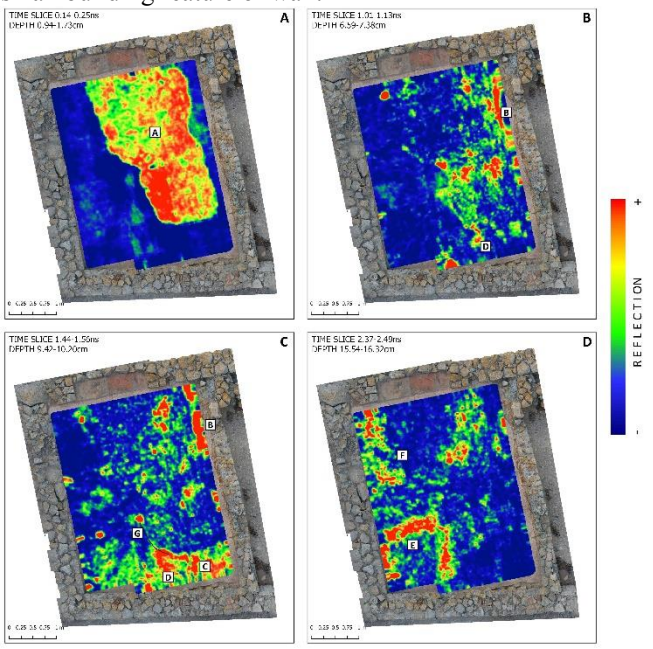

Fig. 3. Sequence of four (A to D) horizontal slices of the Hilbert transformed GPR data cube at different depths showing the presence of seven interpreted features (A to G). Color palette represents the signal amplitude reflection being red the strongest and blue the weakest values respectively.

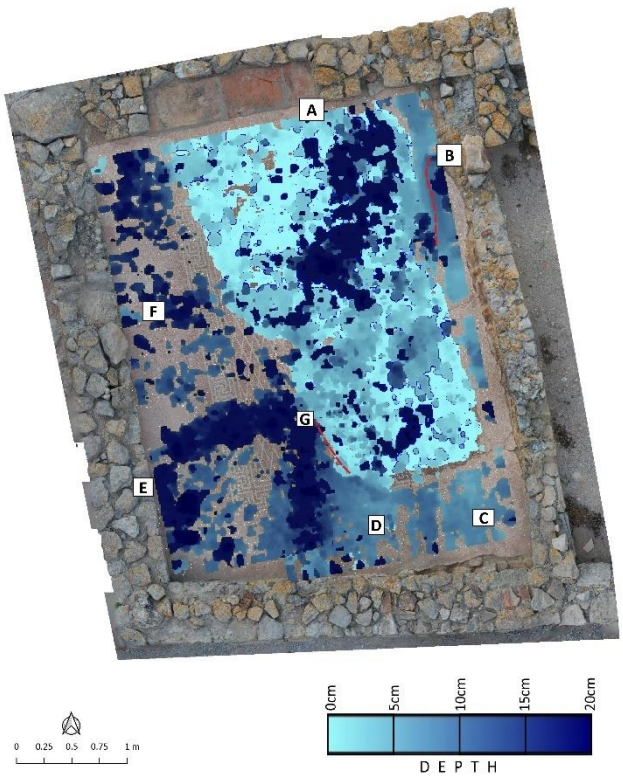

Fig. 4. shows data overlayed in a single image in which only reflectors higher than a 65% amplitude threshold are represented and colour coded according to their depth

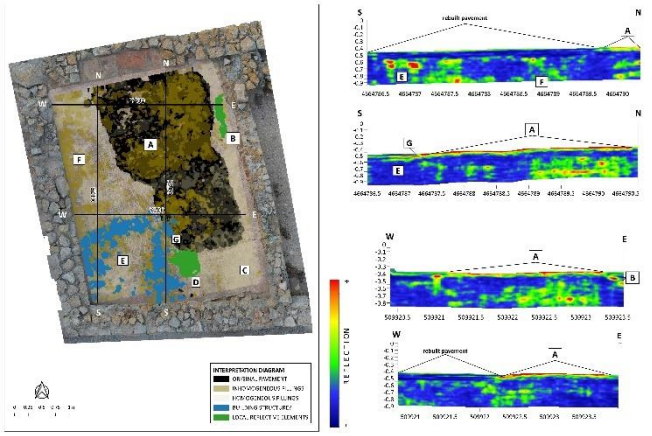

Fig. 5. Left side: Diagram showing interpretation of the different mosaic's pavement layers extracted from GPR data overlay analysis shown in figure 4. Right side: Sections (vertical cuts) in X (S-N) and Y (W-E) directions showing the presence of the interpreted features (A-G).

Due to limited time in the field, more focus on acquiring 3D GPR data over different mosaics and given the fact that UT data collection is slower, only a 1.4m long UT measurement was performed over the bulging area. C-scans at different depths (Fig. 6) show several high amplitude events indicating possible air gaps in the first 25cm. Of particular interest for this investigation are those from 5cm to 15cm depth.

Even if the expected depth of the air gap is shallow and data were highly affected by surfaces waves and coupling effects, the UT results were useful in finding areas with voids that correlate well with damages (bulging) on the surface of the mosaic.

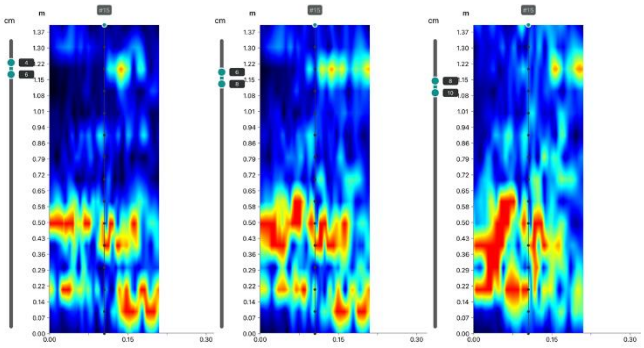

Fig. 6. C-scan data views of ultrasonic (UT) data from 4 to 10cm. Red color events indicate possible air gaps and are coincidental with the bulging area.

V. Discussion

According to the data interpretation, the ancient and rebuilt areas of the pavement show evident differences in their construction methods. While the original pavement seems to lay over a second layer of small rocks and sand, the rebuilt area seems to consist in a mortar pavement laying in a more homogeneous media, probably sand until depths of 8-9cm. The different construction materials of the two regions of the pavement inevitably leads to different mechanical behaviors. This is heavily impacting on the materials' cohesion of both parts of the mosaic. In this regard, the use of beach sand as filling material for the base layer of the rebuilt area can be particularly problematic. The reason is that action of microorganisms in that medium could significantly alter the compaction of the sand layer, and consequently, affect the structural strength of the mosaic. It is plausible therefore to think that this is the main origin of the surface cracks and bulging. However, deformations could also respond to other factors and produce other collateral effects. Water infiltration through surface cracks for example is likely contributing to other damages.

There are plans for a second campaign in order to refine the methodology by using a novel high-frequency multichannel GPR (Proceq GP8100) for quicker 3D scanning together with more UT measurements of selected areas based on these first interpretations. For example, linear features G and B, close to the contact between the old and recent pavements may be small voids that could be verified performing more UT measurements. Measurements under saturated soil conditions are also considered to determine how different moisture levels within the layers of the structure affect the mosaic.

VI. Conclusion

The results of this study show the potential of GPR as an efficient method for monitoring the integrity of historical floors. Popularity of these technologies is growing due to increasing affordability and intuitiveness. Moreover, easy access to 3D GPR data collection is being achieved with new software and hardware capabilities. This is creating rapid adoption for streamlined applications like location of subsurface utilities.

However, data analysis and interpretation of complex sites still requires a high level of expertise. This is yet a bottleneck for other applications to benefit more from GPR technology. For making a difference in the conservation of monumental structures, consistent GPR monitoring would be needed for preventive diagnosis. A more intelligent data analytics software that can automate post-processing steps and assess with interpretation is therefore critical. In addition, further research is yet needed to provide end-users with more qualitative and quantitative information such as: material segmentation or moisture content.

ACKNOWLEDGMENT

The authors would also like to thank (MAC), (Archaeologist, Empuries team).

REFERENCES

[1] ICOMOS https://www.icomos.org/risk/2001/icahm2001.htm

[2] D. Goodman, "Ground-penetrating radar simulation in engineering and archaeology" in Geophysics, vol 59 (2), 1994, pp. 196-202.

[3] L.B.Conyers, Ground-Penetrating Radar for Archaeology. AltaMira Press: Walnut Creek, CA. 2004, 203p.

[4] D. Goodman and S. Piro. "GPR imaging on historical buildings and structures." In GPR Remote Sensing in Archaeology, 2013, pp. 143-157. Springer, Berlin, Heidelberg.

[5] A. Calia, D. Colangiuli, G. Leucci, L. Matera, M. Lettieri, R. Persico and M. Sileo, "Non-destructive and laboratory diagnostic study on the mosaic of the crypt of St. Nicholas (Bari, Italy)," 14th International Conference on Ground Penetrating Radar (GPR), 2012, pp. 579-584, doi: 10.1109/ICGPR.2012.6254930.

[6] E. Utsi, "Target Resolution Using Very High Frequency Ground Penetrating Radar" in Structural Faults and Repair 2014, London, 2014.

[7] B. Caldeira, R. J. Oliveira, T. Teixidó, J. F. Borges, R. Henriques, A. Carneiro, and J. A. Peña, "Studying the Construction of Floor Mosaics in the Roman Villa of Pisões (Portugal) Using Noninvasive Methods: High-Resolution 3D GPR and Photogrammetry" in Remote Sensing 11, no. 16: 1882. https://doi.org/10.3390/rs11161882

[8] N. Linford, P. Linford, L. Martin, A. Payne, "Stepped frequency ground-penetrating radar survey with a multi-element array antenna: Results from field application on archaeological sites" in Archaeological Prospection, vol. 17, 2010, pp. 187-198. doi: 10.1002/arp.382.

[9] L. Sambuelli, C. Comina, G. Catanzariti, F. Barsuglia, G. Morelli, F. Porcelli, "The third KV62 radar scan: Searching for hidden chambers adjacent to Tutankhamun's tomb" in Journal of Cultural Heritage, vol. 39, 2019, pp. 288-296, ISSN 1296-2074,

[10] M. Grasmueck and A. Novo, "3D GPR imaging of shallow plastic pipes, tree roots, and small objects," 2016 16th International Conference on Ground Penetrating Radar (GPR), 2016, pp. 1-6, doi: 10.1109/ICGPR.2016.7572671.

[11] G. Tronca, S. Lehner, L.Raj, I. Tsalicoglou, J. Meier and R. Mennicke, "Looking into concrete – multiple frequency usage in radar products to detect structural parameters and defects faster and more accurately", 2017, 15th Asia Pacific Conference for Non-Destructive Testing (APCNDT2017), Singapore.

[12] M. Rucka, E. Wojtczak and M. Zielińska. "Integrated application of GPR and ultrasonic testing in the diagnostics of a historical floor." Materials 13.11 (2020): 2547.

[13] M.S. Watters - BAR INTERNATIONAL SERIES, 1999 - proceedings.caaconference.org

[14] A. Novo, R. Sala, G. Morelli, J. Leckebusch and J. Tremoleda Trilla, "Full wave-field recording: STREAM X at Empuries (Girona, Spain)" in Archaeological Prospection – 9th International Conference, Drahor MG, Berge MA (eds). Izmir (Turkey), 2011, pp. 213–217.

[15] R. Sala, H. Ortiz-Quintana, E. Garcia-Garcia, P. Castanyer, M. Santos, and J. Tremoleda. "The late-Roman site of Santa Margarida d'Empúries. Combining geophysical methods to characterize a settlement and its landscape." in 12th International Conference of Archaeological Prospection, 2017, p. 199.

[16] D. Goodman, H. Hongo H, N. Higashi, H. Inaoka and Y. Nishimura, "GPR survey over burial mounds: Correcting for topography and the tilt of the GPR antenna" in Near Surface Geophysics, vol. 5, 2007, pp. 383–388.

[17] A. Novo, H. Lorenzo, F. I. Rial and M. Solla. "From pseudo-3D to full-resolution GPR imaging of a complex Roman site" in Near Surface Geophysics, vol. 10, 2012, pp. 11-15.

[18] M. Grasmueck, R. Weger and H. Horstmeyer, "Full-resolution 3D GPR imaging" in Geophysics vol. 70, 2005, pp. K12–K19.

[19] M. Schickert, M. Krause, and W. Müller. "Ultrasonic imaging of concrete elements using reconstruction by synthetic aperture focusing technique." In Journal of materials in civil engineering 15.3, 2003, pp. 235-246.

[20] D. Goodman, J. Steinberg, B. Damiata, Y. Nishimura, K. Schneider, H. Hiromichi and N. Higashi, "GPR overlay analysis for archaeological prospection". Proceedings of the 11th International Conference on Ground Penetrating Radar, Columbus, Ohio, USA, 2006, Expanded Abstracts.